13th South African Conference on Computational and Applied Mechanics (SACAM2024)
22 – 23 January, 2024, Stellenbosch, South Africa

DEVELOPMENT OF A SPILLWAY AND SLUICE GATE DEMONSTRATION SYSTEM

Niël Gertenbach[1*], Jan-Hendrik Kruger[2†]

[*] Presenting author: nielgertenbach@gmail.com
[†]Corresponding author: jandhendrik.kruger@nwu.ac.za
[1,2]North-West University, School of Mechanical Engineering
Private Bag X6001, Potchefstroom, 2520

Abstract: Hydraulic control structures form vital components in modern infrastructure and engineering, from hydroelectric power generation to water storage and canal locks, and they need to be designed appropriately. Mechanical engineering students will benefit from practical exposure to hydraulic control structures supplementing their studies of fluid mechanics. This paper covers the analysis, simulation, and experimental results of a test bench to perform open channel flow demonstrations for engineering education. The flow phenomena incorporated into the designed apparatus were focused on the development of hydraulic jumps in the open channel and the transition from free to submerged flow at a sluice gate opening. CFD simulations using the Volume-Of-Fluids methodology in Ansys Fluent were validated with an analytical model, as both indicated the formation of a hydraulic jump at specific gate openings and flow rates. The effects of three variables were then further characterised during subsequent simulations and experiments, namely the height of the gate opening, the flow rate, and the stop log depth. The testing and construction of the test bench was completed at North West University and demonstrated that the test bench was successful and could be used to investigate other hydraulic structures such as culverts, radial gates, and weirs.

Key words: Hydraulic control structures, sluice gate, computational fluid dynamics, volume-of-fluids

1 Introduction

What is the best way to teach fluid mechanics to undergrad students? Arguably, it is an approach that introduces students to the fundamental fluid flow equations, but in a strong context of practical application [1]. As such, the School of Mechanical Engineering identified the need for a test bench that would allow the practical demonstration of fluid mechanics concepts and open channel flow phenomena, which will add to the theory taught in class.

Therefore, the focus of this study was the development of a test bench that demonstrates the effect of a sluice gate on downstream channel flow. As proof of concept, the formation of a hydraulic jump at specified gate openings, flow rates, and downstream depths was investigated using CFD simulations and experimentally validated.

2 Theory

This section discusses the main equations related to the hydraulic jump and its transition, as used in the current study for analytical validation.

2.1 Hydraulic Jump

A hydraulic jump is the rapid transition in the flow regime from supercritical to subcritical. For example, a spillway gate creates a constriction in the flow path, which causes supercritical flow at the gate opening, which then transitions to subcritical downstream due to flow disturbances. Hydraulic jumps are useful for dissipating the energy of supercritical flow. [2]

Hydraulic jumps can be predicted by investigating the Froude number of a flow region. The Froude number, Fr, is a dimensionless variable that describes how fast a typical wave moves relative to the flow field. When the Froude number is smaller than 1, the flow will be subcritical and supercritical for a Froude number larger than 1. When the Froude number is equal to 1, the flow is critical [2].

The Froude number can be calculated according to [2] as shown in Eqn. (1) where V is the flow velocity, g the gravitational acceleration and y the flow depth.

$$Fr = \frac{V}{\sqrt{gy}} \tag{1}$$

If the Froude number indicates supercritical flow, a hydraulic jump could occur when there is an obstacle that causes a disturbance in flow and a change in the flow regime. With subcritical flows, the depth of the fluid will only change gradually when disturbances or obstacles are encountered. Table 1 shows the hydraulic jump classification for a range of Froude numbers. [2]

Table 1: Hydraulic Jump Classification [2]

Froude Number	Jump Classification
<1	Impossible
1 to 1.7	Standing wave or undulant
1.7 to 2.5	Weak jump
2.5 to 4.5	Oscillating
4.5 to 9	Stable and steady
>9	Rough, strong

When water in the supercritical flow regime encounters, for example, a stop log at the end of a flume, the water will lose velocity and the depth will increase. This region of low-velocity water will cause a hydraulic jump where the two flow regimes meet.

The specific energy equation is used to evaluate open channel flow energy considerations and is shown in Eqn. (2) [2]. Specific energy is especially helpful in investigating the possibility of a hydraulic jump and in predicting the flow depths.

$$E = y + z + \frac{V^2}{2g} \tag{2}$$

Assuming the elevation, z to be zero, Fig. 1 illustrates the relationship between specific energy and flow depth at a constant flow rate of 30 l/min. It shows a sudden turning point at a depth of 0.0173 m and a specific energy of 0.026 m. This turning point corresponds to the critical depth at which the Froude number is one. The arrow shows the determination of a potential hydraulic jump from a depth of 0.006 m to 0.08 m.

According to [3], the critical depth, which is the point at which the specific energy is at its minimum, can be derived from Eqn. (2). This is shown in Eqn. (3) where q is the flow rate per channel width.

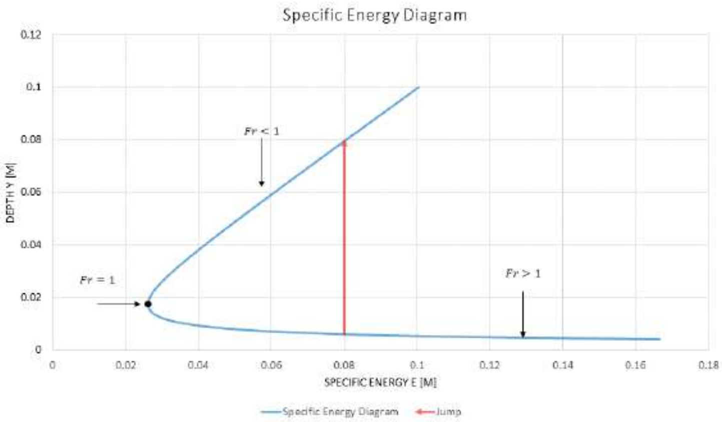

Figure 1: Specific energy as function of flow depth at a constant flow rate

$$y_c = \sqrt[3]{\frac{q^2}{g}} \tag{3}$$

Using Eqn. (3) and a flow rate of 30 l/min, a critical depth of 0.0173 m can be calculated, similar to what was determined from the specific energy diagram.

To calculate the depth of a hydraulic jump, Eqn. (4) can be used, which is derived from the momentum equation when assuming uniform and steady flow, see [2].

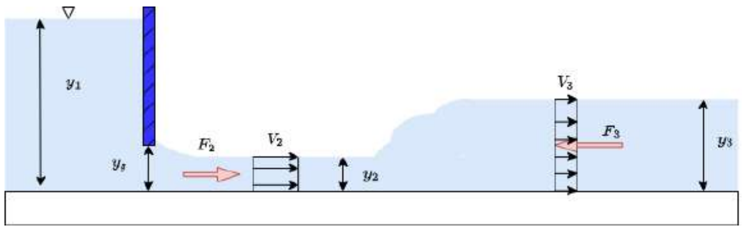

Figure 2: Conservation of momentum over a hydraulic jump. Adapted from [2].

$$\frac{y_3}{y_g} = \frac{1}{2}(-1 + \sqrt{1 + 8Fr_g^2}) \tag{4}$$

2.2 Free or submerged flow transition

The discharge from a spillway gate can be classified as free-flow or submerged-flow. According to [4], free flow will occur when the upstream depth is significantly larger than the gate opening. Submerged flow occurs when the ratio of upstream depth to gate opening is relatively low and will develop when the following conditions are met:

$$y_3 < y_1 < 0.81 y_3 (\frac{y_3}{y_g})^{0.72} \tag{5}$$

2.3 Discharge Coefficient

The discharge of a sluice gate can be determined using Eqn. (6), where C_d is the discharge coefficient. This equation can also be used to determine the upstream depth (y_1) for a given flow rate and gate opening.

$$Q = C_d y_g b \sqrt{2gy_1} \tag{6}$$

The discharge coefficient for the free flow from the sluice gate can be calculated from the various flow depths with Eqn. (7) [4]:

$$C_d = 0.611(\frac{y_1 - y_g}{y_1 + 15y_g})^{0.072} \tag{7}$$

3 Development of test bench

The goal was to develop experimental equipment to demonstrate how theoretical knowledge and principles are applied in real life. This was done by developing an open channel flow test bench with a sluice gate to allow the formation of a hydraulic jump. Water is circulated with a centrifugal pump connected to a sump at the inlet and the channel at the outlet. After flowing through the channel, the water drops back into the sump. Fig. 3 shows the construction of the test bench and some of its components. Fig. 4 shows the actual test bench with a hydraulic jump.

Figure 3: Test Bench Construction

Figure 4: Test bench showing a hydraulic jump in process

4 Experimental methodology

Stop logs are beams that are usually added incrementally to a spillway or channel to seal it and allow maintenance of the spillway or gate. In this experiment, stop logs were used to regulate the depth of the downstream flow. Eight 5 *mm* plexiglass rods were used as stop logs and dropped into a slot at the end of the channel. The water then flowed over the stop logs, and the barrier raised the flow depth.

The following experimental procedure should be followed:

- Switch on the pump and open the valve.
- Allow the flow to stabilise.
- Adjust the opening of the gate (y_g) and the height of the stop logs.
- Allow the flow to stabilise.
- Measure the depth of the hydraulic jump (y_3) and the depth upstream of the gate (y_1).
- Repeat the measurements three times to obtain a dataset.

The hydraulic jump depth was determined analytically using Eqn. (4), and adding the height of the stop logs. The depth upstream of the gate was analytically determined using Eqn. (6).

The values of the analytical equations were then compared to the actual measurements as part of the validation process.

5 Simulation methodology

CFD simulations were conducted to serve as an additional tool along with analytical calculations to verify the design and operation of the test bench. Simulations were performed using Ansys Fluent, release 2023R1, with multiphase modelling.

The simulations were conducted in two dimensions since no elements changed along the width of the channel and to save computational time. The simulation operating conditions were atmospheric and steady state. The standard multiphase volume-of-fluid (VOF) model was used to represent the interaction between water and air and to provide a solution for the interface between these, in other words, to calculate the movement of the surface of the water.

The VOF method uses a continuum indicator function (α) to represent the various fluids contained in the model domain. It typically has a value of zero in regions completely occupied by the first fluid and a value of one for regions occupied by the second fluid. In the interface region between the two fluids, the indicator function varies between one and zero, that is, $0 < \alpha < 1$. Using the indicator function as a weighting factor, the fluid properties of the mixture can then be determined, e.g. the density function shown in Eqn. (8).

$$\rho = \alpha \cdot \rho_1 + (1 - \alpha) \cdot \rho_2 \tag{8}$$

The momentum and energy conservation equations are then solved according to the standard SIMPLE-C algorithm, but using the weighted properties of the fluid mixture instead of only one fluid [5]. Second-Order Upwind discretization was used to achieve second-order accuracy, and a least squares cell-based interpolation method (gradient) was used as it is less computational intensive, but the same accuracy as the more computational intensive Green-Gauss Node-Based interpolation method. .

The standard k-ε turbulence model was chosen and is suitable for turbulent flows that occurred in the channel. The mesh dependency was not fully investigated, as the mesh resolution was already at the finest that the available computer could handle. The maximum iterations were set at 1000, but convergence often occurred earlier.

Fig. 5 shows the Spaceclaim model used in the CFD simulations, and the important elements of the model are also indicated. The flow straightener was added to impart uniform flow, and a buffer plate was used to reduce the incoming velocity.

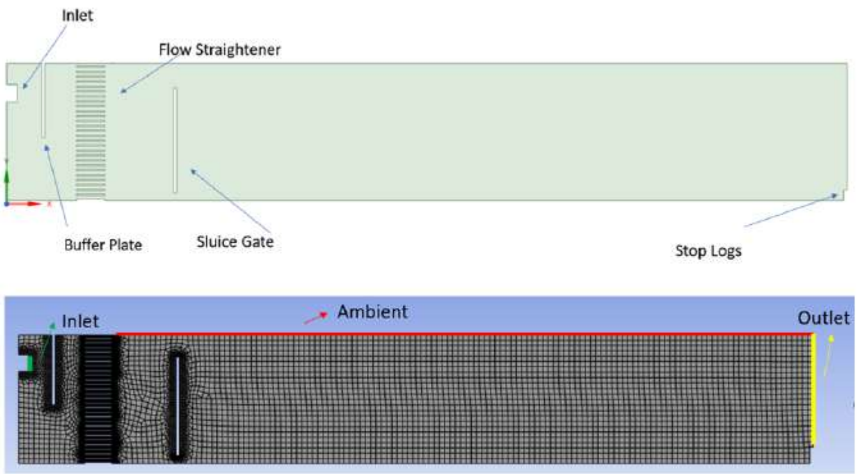

Figure 5: Simulation model and mesh. **Top:** Spaceclaim CAD model. **Bottom:** Simulation mesh showing local refinement and boundary conditions.

The CFD mesh is shown at the bottom of Fig. 5 and indicates the different boundary conditions of the channel. The top section from the inlet to the end of the flow straightener was closed to keep water from splashing out, but it was open to the atmosphere at the ”Ambient” edge. Local mesh refinement was employed around the buffer plate, flow straightener, and sluice gate components to capture fine details of the highly complex flow in those regions.

6 Results

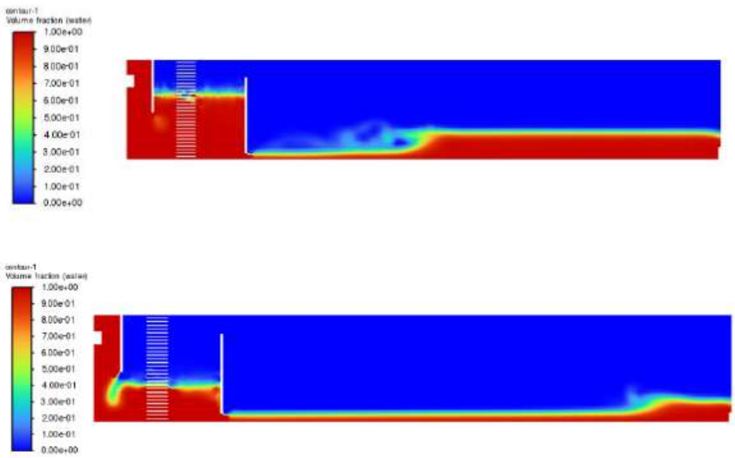

Figure 6: Hydraulic jump formation under different conditions. **Top:** Gate opening of 12 *mm* with 15 *mm* stop logs. **Bottom:** Gate opening of 15 *mm* with 10 *mm* stop logs.

Fig. 6 show the results of the simulation carried out at a flow rate of 50 l/min, with 12 and 15 *mm* gate openings, and stop log heights of 15 and 10 *mm*, respectively. The blue region represents air, and the red region represents water. The sudden increase in flow depth indicates a hydraulic jump. It can be seen that with fewer stop logs (therefore, lower flow resistance), the hydraulic jump occurs later in the stream.

Fig. 7 shows the influence of the height of the stop logs on the depth of the hydraulic jump (y_3) at a flow rate of 73 l/min and a gate opening (y_g) of 20 *mm*. The height of the stop logs was incrementally increased from 0 to 40 *mm*. The inconsistency at the lower gate openings was due to the hydraulic jump

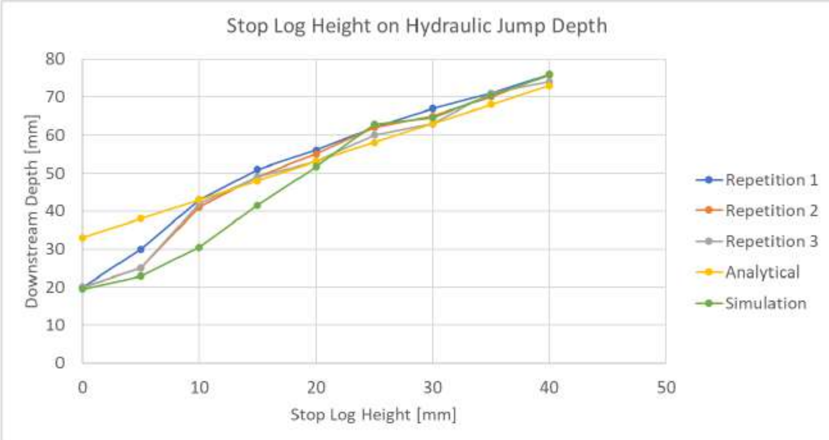

Figure 7: Hydraulic jump depth as function of stop log height. (Gate opening of 20 *mm* and flow rate of 73 l/min.)

not developing within the channel length. With the increase in the height of the stop logs, the hydraulic jump was pushed upstream. Fig. 7 also shows that the simulation results were initially lower. This is possibly due to the 2D nature of the simulations, where wall friction cannot be accounted for. With lower frictional resistance in the channel, the disturbance required to trigger a hydraulic jump increased. Hydraulic jumps therefore often occurred at slightly higher stop log heights in the simulations than during the experiments.

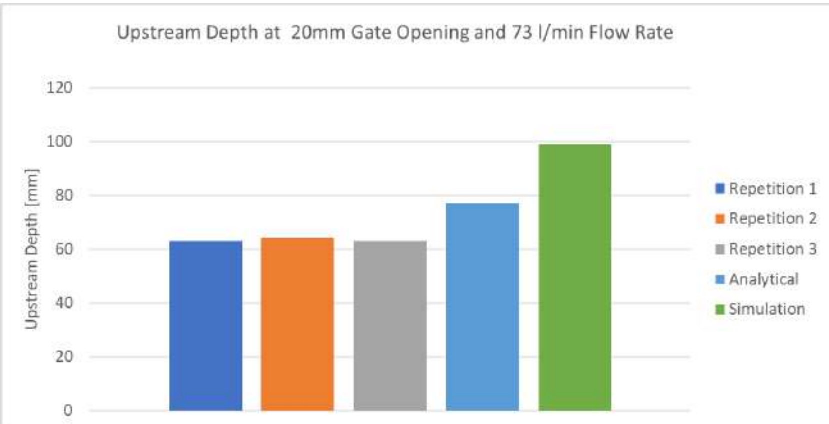

Figure 8: Results for depth upstream of the gate. (Gate opening of xx *mm* and flow rate of xx l/min.)

Fig. 8 shows a comparison of computational, simulation, and analytical results for flow depth (y_1) upstream of the gate. Analytical results were obtained using Eqn. (6). It shows that the test bench delivered repeatable results, but 18% lower than the analytical results. This deviation is suspected to be due to small leaks present between the gate and the channel walls.

The results of the simulation were comparably higher than the analytical and experimental values. The higher depth predicted by the simulations was possibly due to (1) the absence of leakage flow effects in the CFD model and (2) how the flow straightener, used to impart uniform flow, was modelled in 2D, which was not an exact representation of the actual 3D device on the test bench.

Whether the discharge from the sluice gate was submerged or free also influenced the formation of the hydraulic jump. The submerged flow lowers the velocity, which subsequently lowers the Froude number of the flow. If the velocity is lowered enough, the discharged flow will be sub-critical, making a hydraulic jump impossible.

Submerged flow was experienced when the stop logs were too high and pushed the hydraulic jump upstream up to the gate, and at low flow rates, which required an extremely small gate opening to achieve supercritical flow.

An experiment was conducted to investigate the transition from free flow to submerged flow as a result of the increase in the stop log height. It was carried out with a gate opening of 20 *mm*, a flow rate of 116 l/min, and an incremental increase in the height of the stop log. Fig. 9 shows the upstream depth and the right-hand side (RHS) of Eqn. (5). The intersection between the upstream depth and the RHS is the point where the transition occurred. When the RHS is greater than the upstream depth, the flow is submerged. As expected, the depth upstream (y_1) of the gate also increased as the flow became submerged.

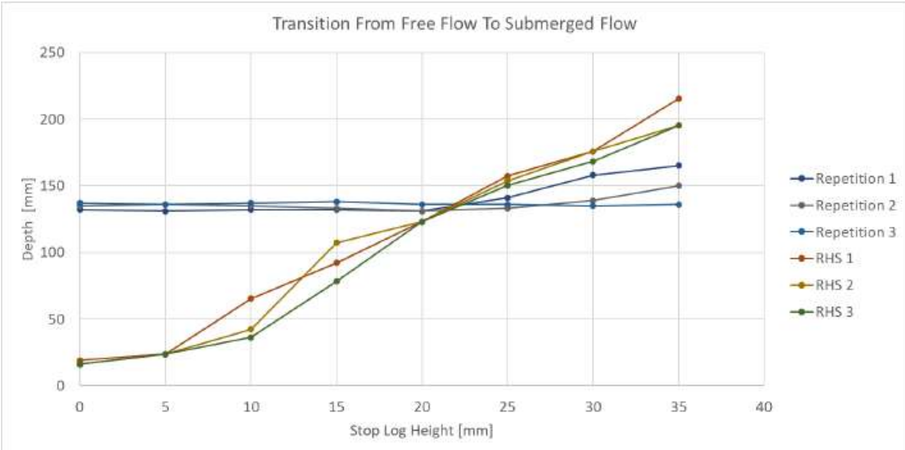

Figure 9: Experimental results showing transition from free to submerged flow, related to variations in the stop log height. (Gate opening of 20 *mm* and flow rate of 116 l/min.)

7 Conclusion

During the experiments, it was observed that lower gate openings lead to a stronger hydraulic jump as a result of the higher discharge velocity and also moved the jumps downstream. More stop logs moved the jump upstream, and higher flow rates moved the jump downstream, and they also had stronger jumps.

The test bench was successful in demonstrating open-channel flow geometries and regimes, the development of a hydraulic jump, similarity to analytical calculations, the transition from free to submerged flow, and the upstream and downstream shifting of a hydraulic jump.

The test bench does have a few practical limitations, which include not having a real time flow measurement device, unmeasured friction due to the silicon used to seal the channel, manual gate operation, slight leaking between the gate and the channel walls, and lastly the small operating range due to the short length of the channel.

The simulations showed encouraging agreement with experimental results, but may be improved by developing a full 3D model to fully incorporate wall friction effects and the 3D effects of the flow straightener. A more extensive numerical investigation may also be performed to explore the effects of the interface capture scheme used in the VOF method to determine whether it has a significant effect on the prediction of the height and location of the hydraulic jump.

Nomenclature

α	Density indicator function	–
γ	Specific weight of water	$\frac{N}{m^3}$

ρ	Density	$\frac{kg}{m^3}$
C	Discharge coefficient	–
E	Energy head	m
Fr	Froude number	–
H	Water head	m
Q	Volume flow rate	$\frac{l}{min}$
q	Specific flow rate	–
R_h	Hydraulic radius	m
Re	Reynolds number	–
V	Velocity	m/s

Acknowledgement

I wish to thank the Lord for blessing me with my skills, for guidance and discipline. I wish to also thank Dr. Kruger for his guidance on this project, as well as my parents who funded my studies and exposed me to the wonderful world of engineering. I also acknowledge Marinique for her support and motivation.

References

[1] Ashwin Vaidya. "Contributions to the Teaching and Learning of Fluid Mechanics". In: *Fluids* 6 (July 2021), pp. 269–269. DOI: 10.3390/fluids6080269. URL: https://www.mdpi.com/2311-5521/6/8/269/htm (visited on 12/10/2023).

[2] B.R. Munson et al. *Fluid Mechanics*. 7th. Wiley & Sons, 2013.

[3] M. Hanif Chaudhry. *Open-Channel Flow*. 2nd ed. Springer, 2008. URL: https://link.springer.com/book/10.1007/978-0-387-68648-6 (visited on 08/15/2023).

[4] Prabhata K. Swamee. "Sluice-Gate Discharge Equations". In: *Journal of Irrigation and Drainage Engineering* 118 (1992), pp. 56–60. URL: https://www.academia.edu/45391822/Sluice_Gate_Discharge_Equations (visited on 08/13/2023).

[5] ANSYS Incorporated. *Introduction to ANSYS FLUENT*. Dec. 2010. URL: https://imechanica.org/files/fluent_13.0_lecture05-solver-settings.pdf.